

# The Discovery of Conformationally Constrained Bicyclic Peptidomimetics as Potent Hepatitis C NS5A Inhibitors

Wieslaw M. Kazmierski,<sup>\*,#</sup> Nagaraju Miriyala,<sup>#</sup> David K. Johnson, and Sam Baskaran



Cite This: *ACS Med. Chem. Lett.* 2021, 12, 1649–1655



Read Online

ACCESS |



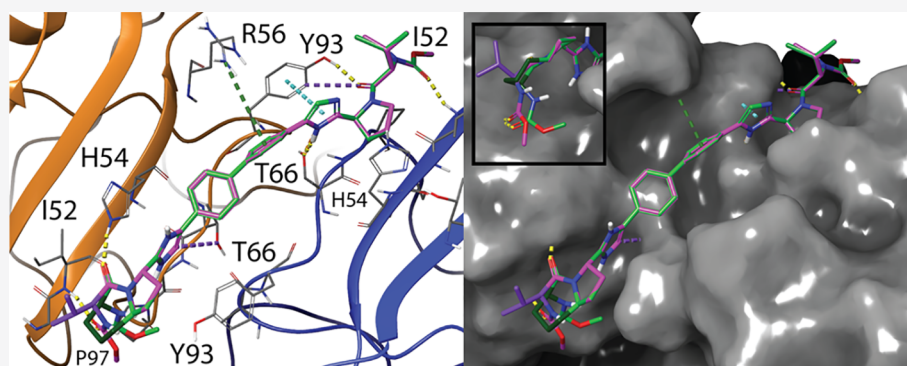
Metrics & More



Article Recommendations



Supporting Information



**ABSTRACT:** HCV NS5A inhibitors are the backbone of directly acting antiviral treatments against the hepatitis C virus (HCV). While these therapies are generally highly curative, they are less effective in some specific HCV patient populations. In the search for broader-acting HCV NS5A inhibitors that address these needs, we explored conformational restrictions imposed by the [7,5]-azabicyclic lactam moiety incorporated into daclatasvir (**1**) and related HCV NS5A inhibitors. Unexpectedly, compound **5** was identified as a potent HCV genotype 1a and 1b inhibitor. Molecular modeling of **5** bound to HCV genotype 1a suggested that the use of the conformationally restricted lactam moiety might have resulted in reorientation of its N-terminal carbamate to expose a new interaction with the NS5A pocket located between amino acids P97 and Y93, which was not easily accessible to **1**. The results also suggest new chemistry directions that exploit the interactions with the P97–Y93 site toward new and potentially improved HCV NS5A inhibitors.

**KEYWORDS:** HCV, hepatitis C virus, genotype 1a, genotype 1b, nonstructural protein 5A, HCV inhibitor

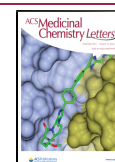
The hepatitis C virus (HCV) is a 9.6 kb positive-strand RNA virus that can cause chronic liver disease, cirrhosis, and hepatocellular carcinoma (primary liver cancer). The World Health Organization estimated that at least 170 million people worldwide were infected with HCV and that in 2016 about 400 000 people died from hepatocellular carcinoma.<sup>1</sup> HCV is a blood-borne virus that is transmitted primarily through unsafe injection practices, transfusion of unscreened blood, and unsafe sexual contacts. The HCV genome contains seven genotypes (1–7) and more than 90 subtypes and encodes 10 proteins, some structural (core, E1 glycoprotein, E2) and some nonstructural (p7, NS2, NS3, NS4A, NS4B, NS5A, NS5B).<sup>2,3</sup> The NS5A protein, which is active as a homodimer, consists of three domains, of which domain 1 is the most structured and essential for HCV genome replication.<sup>4</sup> The FDA-approved dual, triple, and quad regimens combine NS5A inhibitors with other directly acting agents (DAAs) and provide high levels of virologic cure in most patients.<sup>5,6</sup> However, these treatments are less effective in patients with cirrhosis, in genotype 1a (gt1a) patients undergoing interferon-free treatment, and in interferon non-

responders, thus arguing for the continued need to discover improved pharmaceutical options for these populations.<sup>7–9</sup>

We previously reported the discovery of the clinical NS5A inhibitor GSK2336805 (JNJ-5614845) and the conformationally constrained NS5A inhibitor GSK2818713 (Figure 1).<sup>6,10,11</sup> Conformational constraints can enhance potency and reduce metabolic liability.<sup>10a,12</sup> In a continued effort to explore this approach toward discovery of improved HCV NS5A inhibitors, we decided to incorporate the [7,5]-azabicyclic lactam motif as a dipeptide mimetic into **1** and related compounds and synthesized analogues **2–13** (Tables 1–3 and Schemes 1–3).<sup>12,13a–e,14</sup>

Received: July 17, 2021

Published: September 15, 2021



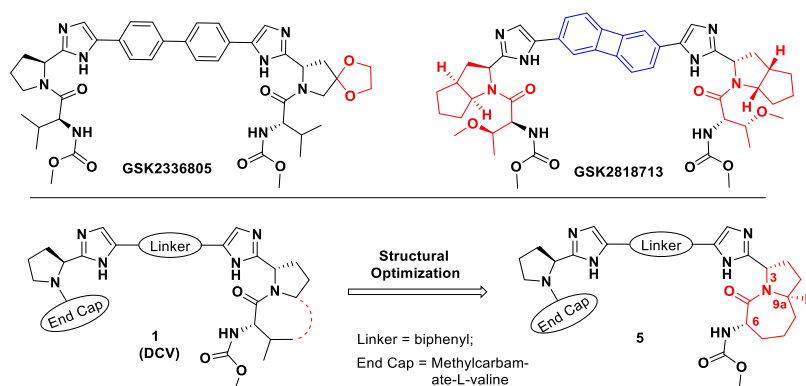


Figure 1. Conversion of 1 into bicyclic 5.

With fixed position 3*S*, four sets of diastereomers were produced to explore the effect of both *R* and *S* chirality at positions 6 and 9*a* on the potency in the HCV replicon assay (Figure 1 and Table 1). Compared with daclatasvir (1), the

Table 1. SAR of Bicyclic Compounds 2–5

Entry	Structure	Huh-luc/neo-ET replicon cells EC <sub>50</sub> [nM] <sup>a</sup>				
		gt1b	gt1a	3	6	9 <i>a</i>
1		0.032	0.079			
2		0.109	17.44	<i>S</i>	<i>S</i>	<i>S</i>
3		0.133	12.48	<i>S</i>	<i>R</i>	<i>S</i>
4		0.059	0.673	<i>S</i>	<i>R</i>	<i>R</i>
5		0.037	0.471	<i>S</i>	<i>S</i>	<i>R</i>

<sup>a</sup>All values are averages of at least three independent experiments.

potency of 2 (6*S*,9*a**S*) decreased slightly against gt1b and significantly (~221-fold) against gt1a. A similar potency profile was observed for 3 (6*R*,9*a**S*), but isomer 4 (6*R*,9*a**R*) regained gt1a and gt1b potency compared with 2 (~27-fold and ~2-fold, respectively). These gains were further enhanced in inhibitor 5 (6*S*,9*a**R*), which was essentially equipotent to 1 against gt1b and only ~6 times less potent against gt1a. The finding that 5 was a subnanomolar HCV inhibitor contrasted with data published elsewhere after our work was completed,<sup>13f</sup> which prompted us to disclose details of our discoveries.

Another interesting finding is that while *R* chirality at position 9*a* is required for high gt1a potency, the chirality at

position 6 turned out to be much less consequential, which contrasts with the well-established structure–activity relationship (SAR) in the linear (1) series, where *S* chirality is required (Table 1). Such divergent SARs can indicate a profound conformational change in the bicyclic series (see Modeling Studies).<sup>15</sup>

The lactam-imposed constraints were further evaluated on the framework of two other NS5A inhibitors. GSK2236805 (gt1b EC<sub>50</sub> = 0.011 nM and gt1a EC<sub>50</sub> = 0.010 nM; Figure 1) has a superior potency profile compared with 1 resulting from interactions of the ketal moiety with NS5A.<sup>10a</sup> Compared with GSK2236805, bicyclic inhibitors 6–9 exhibited slight potency loss on gt1b and a significant one on gt1a (Table 2).<sup>10</sup> Similar to the SAR of 2–5, the 6*R*,9*a**R* isomer (8) and the 6*S*,9*a**R* isomer (9) exhibited the best potency against HCV gt1a.

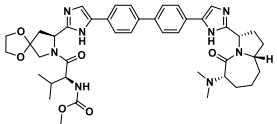
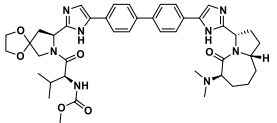
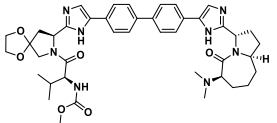
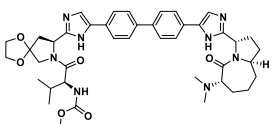
In another very potent series, where the carbamate moiety is replaced with a tertiary amine,<sup>16</sup> the SAR of resulting lactams 10–13 again mirrored the one observed for 2–5, with 13 (6*S*,9*a**R*) being the most potent in this group (Table 3).<sup>11,16</sup> The absolute potencies in this series were lower than for 2–9, (e.g., 13 was 16-fold less potent than 5 against gt1a).

Table 2. SAR of Bicyclic Compounds 6–9

Entry	Structure	Huh-luc/neo-ET replicon cells EC <sub>50</sub> [nM] <sup>a</sup>				
		gt1b	gt1a	3	6	9 <i>a</i>
6		0.046	8.581	<i>S</i>	<i>S</i>	<i>S</i>
7		0.08	14.52	<i>S</i>	<i>R</i>	<i>S</i>
8		0.047	0.707	<i>S</i>	<i>R</i>	<i>R</i>
9		0.064	1.524	<i>S</i>	<i>S</i>	<i>R</i>

<sup>a</sup>All values are averages of at least three independent experiments.

Table 3. SAR of Bicyclic Compounds 10–13

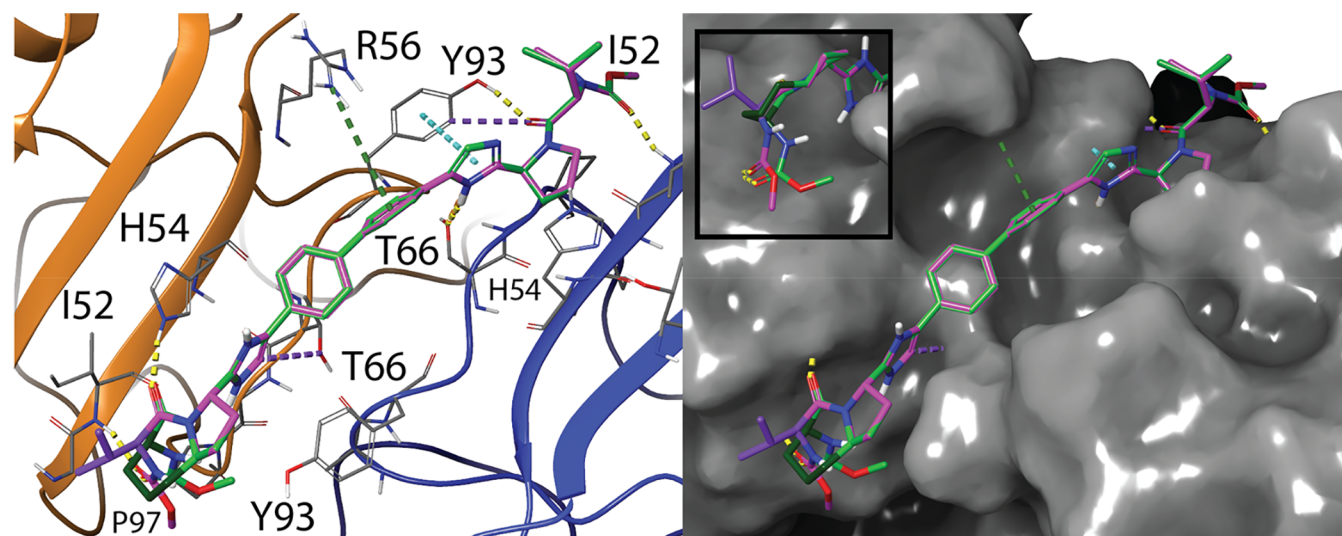
Entry	Structure	Huh-luc/neo-ET replicon cells EC <sub>50</sub> [nM] <sup>a</sup>				
		gt1b	gt1a	3	6	9a
10		0.209	32.165	S	S	S
11		0.217	119.15	S	R	S
12		0.298	10.635	S	R	R
13		0.084	7.707	S	S	R

<sup>a</sup>All values are averages of at least three independent experiments.

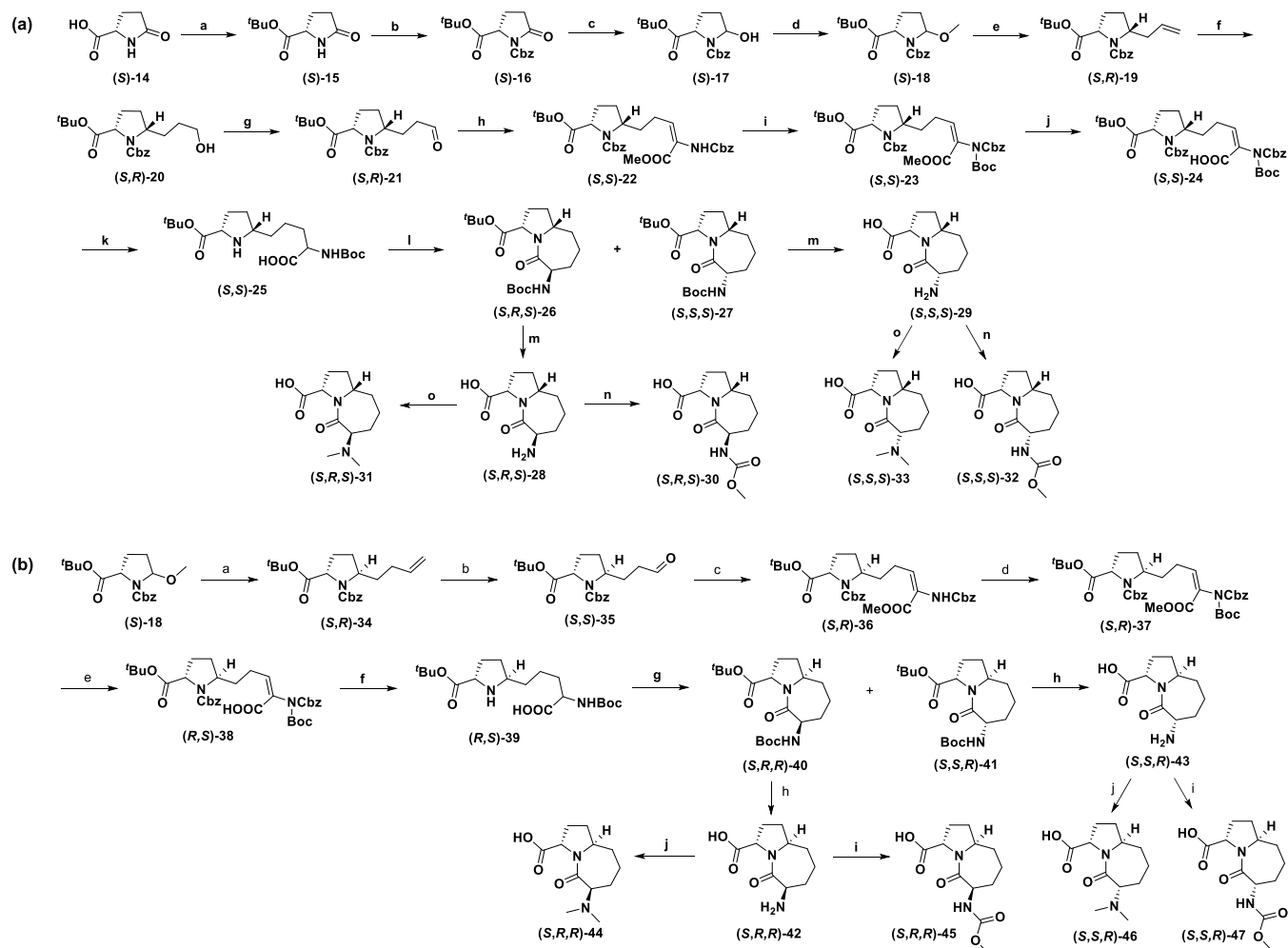
**Modeling Studies.** To rationalize the impact of the bicyclic constraints, we performed molecular modeling studies of analogues. The published structures of NS5A genotypes 1a (PDB ID 4CL1)<sup>17</sup> and 1b (PDB ID 3FQQ)<sup>18</sup> were used to generate models of NS5A in two dimeric states, and their interactions with **1** and **5** were modeled using the docking software Glide.<sup>19–22</sup> The generated low-energy poses, in which **5** had the expected higher (worse) docking score than **1** to gt1a NS5A protein (−6.925 vs −7.737 kcal/mol, respectively), were consistent with the experimental data. The most

significant difference between **1** and **5** docked to gt1a appears to be the loss of favorable hydrophobic interactions between the isopropyl of **1** and I52 of NS5A (Figure 2, bottom left of each panel and inset). Another consequence of the new conformational preference in **5** is reorientation of its methyl carbamate group away from the typically utilized solvent-exposed edge of P97 inward toward a hydrophobic cleft located between P97 of one monomer and Y93 of the other. This pocket is not easily accessible and thus is not utilized by the low-energy conformers of **1** (Figure 2, inset). The interaction of carbamate **5** with the new site is unoptimized, and further chemical modifications of **5** should improve its potency. For example, modeling showed that replacement of the carbamate in **5** with phenyl, difluorophenyl, thiophene, and pyrrole amides significantly increased the affinity of such compounds, as shown by their lower (improved) docking scores versus **1** (−8.434, −8.523, −8.166, and −7.989 vs −7.737 kcal/mol, respectively), as a result of optimized interactions of the aromatic groups with P97–Y93 (Supplemental Figure 1). On the other hand, modeling of the same amides replacing the methyl carbamate in **1** indicated that they were not able to interact strongly with the P97–Y93 pocket, as reflected by their higher docking scores vs the same amides in the bicyclic series (−7.024 vs −8.434, −6.883 vs −8.523, −7.544 vs −8.166, and −7.567 vs −7.989 kcal/mol for the phenyl, difluorophenyl, thiophene, and pyrrole amides, respectively; Supplemental Table 1).

**Syntheses.** Syntheses of [7,5]-Fused Bicyclic Acids **30–33** and **44–47**. The [7,5]-fused *cis*-bicyclic acids **30–33** were synthesized from (*S*)-5-oxopyrrolidine-2-carboxylic acid **14** (Scheme 1a).<sup>23,24</sup> Briefly, **14** was converted to its *tert*-butyl ester **15** with <sup>t</sup>BuOAc and HClO<sub>4</sub>, after which the −NH group was Cbz-protected and the amide was reduced with LiBHET<sub>3</sub> to yield alcohol **17** in 62% yield. **17** was then converted into methoxy derivative (*S*)-**18** with TsOH/MeOH. The requisite *cis*-allyl intermediate (*S,R*)-**19** was secured by allylation of (*S*)-



**Figure 2.** Model of compounds **1** and **5** bound to gt1a. Compounds **1** (magenta) and **5** (green) are modeled to bind at the dimeric interface of gt1a (cartoons and stick, left; surface representation, right). The backbone cartoons are colored by chain. While the common substructures have the same pose and make the same interactions (hydrogen bonds are represented as yellow dashes, aromatic hydrogen-bonding interactions as magenta dashes,  $\pi$ – $\pi$  interactions as cyan dashes, and cation– $\pi$  interactions as green dashes), the bicyclic moiety is modeled to interact differently. The inset features an alternate projection of the bicyclic ring to highlight the loss of interaction between the isopropyl group (darker magenta) and I52 modeled with compound **1** while showing that the bicyclic ring (dark green) constrains the methyl group of the carbamate of compound **5** into a new orientation inward toward the P97–Y93 pocket.

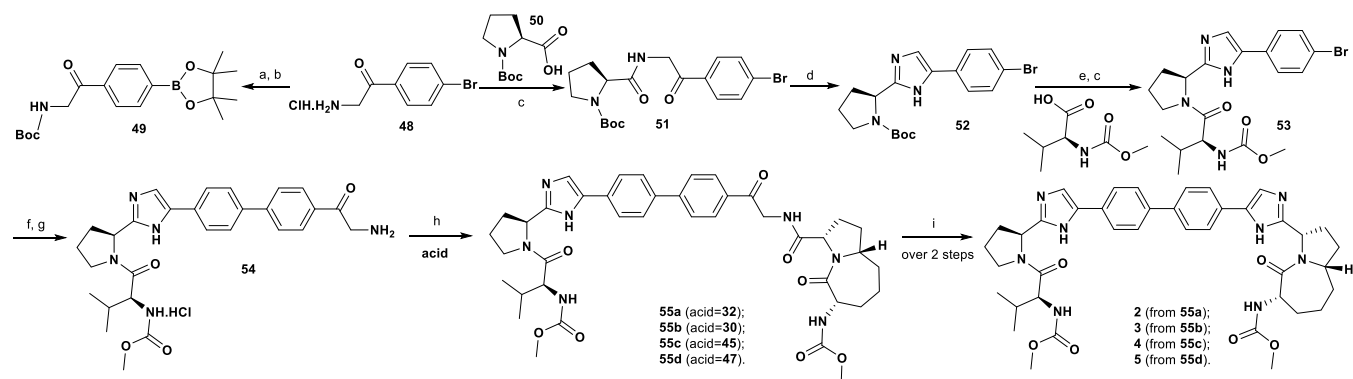
Scheme 1. Syntheses of (a) [7,5]-Fused *cis*-Bicyclic Acids 30–33<sup>a</sup> and (b) [7,5]-Fused *trans*-Bicyclic Acids 44–47<sup>b</sup>

<sup>a</sup>Reagents and conditions: (a) HClO<sub>4</sub>, <sup>t</sup>BuOAc, rt, 12 h, 50%; (b) (i) NaH, THF, 0 °C, 1 h, (ii) Cbz-Cl, rt, 12 h, 50%; (c) LiBHET<sub>3</sub>, THF, –78 °C, 1 h, 63%; (d) TsOH, MeOH, rt, 24 h, 52%; (e) allyltributylstannane, BF<sub>3</sub>·OEt<sub>2</sub>, –78 °C to rt, 3 h, 18%; (f) (i) 9-BBN, THF, rt, 12 h, (ii) H<sub>2</sub>O<sub>2</sub>, 3 N NaOH, rt, 2 h, 81%; (g) PCC, CH<sub>2</sub>Cl<sub>2</sub>, rt, 2 h, 80%; (h) (i) (±)-benzyloxycarbonyl- $\alpha$ -phosphonoglycine trimethyl ester, <sup>t</sup>BuOK, CH<sub>2</sub>Cl<sub>2</sub>, –78 °C, 30 min, (ii) aldehyde, CH<sub>2</sub>Cl<sub>2</sub>, –78 °C, 4 h, rt, 12 h, 88%; (i) Boc<sub>2</sub>O, THF, DMAP, rt, 12 h, 90%; (j) 1 N NaOH, MeOH, rt, 12 h, 66%; (k) Pd/C, MeOH, H<sub>2</sub>, rt, 4 h, quant.; (l) EDC, HOBT, Et<sub>3</sub>N, DMAP, CH<sub>2</sub>Cl<sub>2</sub>, rt, 12 h, 37–39%; (m) TFA, CH<sub>2</sub>Cl<sub>2</sub>, rt, 2 h, quant.; (n) methyl chloroformate, dioxane, 1 N NaOH, rt, 12 h, 85–88%; (o) HCHO, 1 N HCl, Pd/C, MeOH, H<sub>2</sub>, rt, 12 h, 64%. <sup>b</sup>Reagents and conditions: (a) (i) 4-bromobut-1-ene, Mg, THF, reflux, 1.5 h, (ii) CuBr·Me<sub>2</sub>S, THF, –78 °C, 2.5 h, 55%; (b) NaIO<sub>4</sub>, THF, H<sub>2</sub>O, OsO<sub>4</sub>, rt, 2 h, 83%; (c) (i) (±)-benzyloxycarbonyl- $\alpha$ -phosphonoglycine trimethyl ester, <sup>t</sup>BuOK, CH<sub>2</sub>Cl<sub>2</sub>, –78 °C, 30 min, (ii) aldehyde, CH<sub>2</sub>Cl<sub>2</sub>, –78 °C, 4 h, rt, 12 h, 86%; (d) Boc<sub>2</sub>O, THF, DMAP, rt, 12 h, 87%; (e) 1 N NaOH, MeOH, rt, 12 h, 80%; (f) Pd/C, MeOH, H<sub>2</sub>, rt, 4 h, 93%; (g) EDC, HOBT, Et<sub>3</sub>N, DMAP, CH<sub>2</sub>Cl<sub>2</sub>, rt, 12 h, 23–25%; (h) TFA, CH<sub>2</sub>Cl<sub>2</sub>, rt, 2 h, quant.; (i) methyl chloroformate, dioxane, 1 N NaOH, rt, 12 h, 43–54%; (j) HCHO, 1 N HCl, Pd/C, MeOH, H<sub>2</sub>, rt, 12 h, 60–80%.

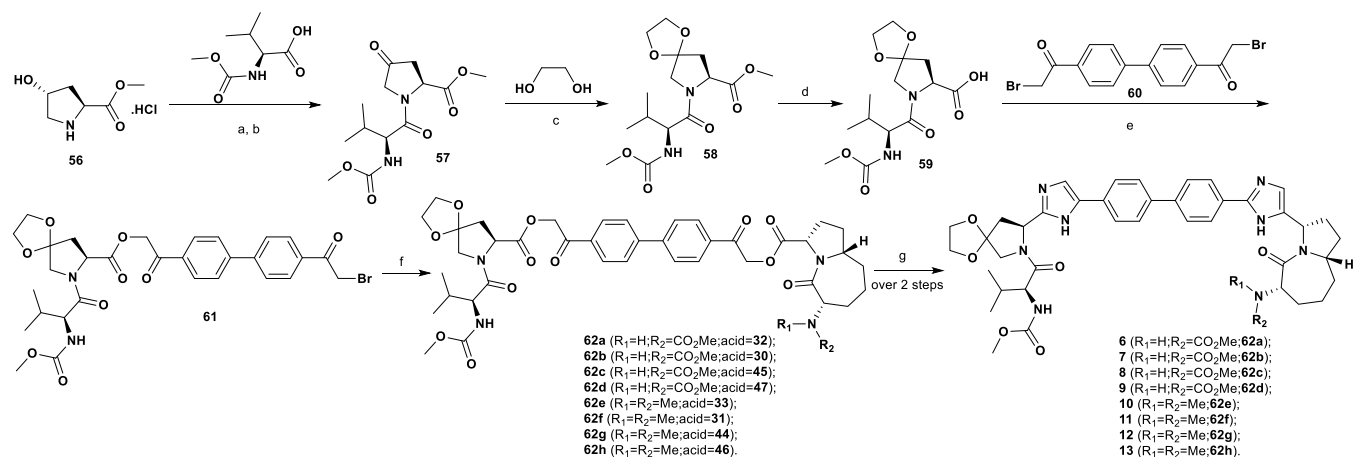
18 with allyltributylstannane/BF<sub>3</sub>·OEt<sub>2</sub>, and 9-BBN-mediated hydroboration of the allyl moiety in (S,R)-19 and subsequent oxidation furnished alcohol 20 in 81% yield. Oxidation of 20 using PCC afforded the key intermediate *cis*-aldehyde 21 in 80% yield, and subsequent Horner–Emmons olefination with (±)-benzyloxycarbonyl- $\alpha$ -phosphonoglycine trimethyl ester furnished 22 in 89% yield. Boc protection of the Cbz carbamate and hydrolysis of 23 afforded acrylic acid 24. Catalytic hydrogenation of 24 and cyclization of 25 gave a 1:1 mixture of diastereomers, which could be separated to yield the desired pure bicyclic (S,R,S)-26 and (S,S,S)-27 (dr > 98%).<sup>24</sup> Deprotection of 26 and 27 to obtain the respective amines 28 and 29 was then followed by their conversion to carbamates 30 and 32, whereas *N,N*-dimethyl-substituted 31 and 33 were obtained by reductive alkylation of 28 and 29, respectively, with formaldehyde. The overall yields for 30–33 were 0.12–

0.17% over 14 steps from 14. The *trans*-bicyclic acid diastereomers 44–47 were synthesized in a similar fashion (dr > 98%) (Scheme 1b).<sup>23,24</sup> Key intermediate *trans*-(S,R)-34 was obtained by reacting (S)-18 with 4-bromobut-1-ene/Mg and CuBr·Me<sub>2</sub>S, paving way for the syntheses of *trans*-bicyclic (S,R,R)-44, (S,R,R)-45, (S,S,R)-46, and (S,S,R)-47 in overall yields of 2.5–5.1% over nine steps from 18.

**General Syntheses of Bicyclic Inhibitors 2–5.** Inhibitors 2–5 were synthesized in 1.2–5.3% overall yield in eight steps starting from 48<sup>10a</sup> by coupling of amine 54 with bicyclic acids 32, 30, 45, and 47 (Scheme 1) followed by imidazole cyclization (Scheme 2) as described in our previous work.<sup>10a</sup> Attempts to couple amine 54 with the bicyclic acids required T3P as a coupling agent to secure 55a–55d, which were then subjected to imidazole cyclization to yield targets 2–5.

Scheme 2. Synthesis of Bicyclic Inhibitors 2–5<sup>a</sup>

<sup>a</sup>Reagents and conditions: (a) 1,4-dioxane, Et<sub>3</sub>N, Boc<sub>2</sub>O, 64%; (b) dioxane, Pd(dppf)Cl<sub>2</sub>, bis(pinacolato)diboron, CH<sub>3</sub>COOK, 58%; (c) CH<sub>2</sub>Cl<sub>2</sub>, HATU, DIEA, 61%; (d) NH<sub>4</sub>OAc, dioxane, 110 °C, 48 h or microwave, 160 °C, 20 min, 89%; (e) HCl(aq), 90%; (f) DME, NaHCO<sub>3</sub>, Pd(dppf)Cl<sub>2</sub>, 18 h, 80 °C, 49, 54%; (g) HCl(aq), quant.; (h) T3P, TEA; (i) NH<sub>4</sub>OAc, microwave, 140 °C, 30 min, 7–30%.

Scheme 3. Synthesis of Spiroketal Bicyclic Inhibitors 6–13<sup>a</sup>

<sup>a</sup>Reagents and conditions: (a) HATU, Et<sub>3</sub>N, 70%; (b) Dess–Martin periodinane, 20%; (c) tosic acid, 44%; (d) LiOH, THF–water–MeOH, 91%; (e) DMF, NaH, rt, 15 min, Et<sub>3</sub>N, quant.; (f) acid, Et<sub>3</sub>N, ACN, 50 °C, 2 h; (g) NH<sub>4</sub>OAc, dioxane, microwave, 145 °C, 40 min, 25–37%.

**General Syntheses of Bicyclic Inhibitors 6–13.** Compounds 6–13 were synthesized analogously to 2–5 in overall yields of 1.4–2.1% starting from 56 (Scheme 3).<sup>10a,11e</sup> Coupling of intermediate 61 with sterically hindered bicyclic acids (32, 30, 45, and 47) required elevated temperatures (50 °C) to furnish the desired amides 62a–h, and subsequent imidazole cyclization secured 6–13.

In the search for improved HCV NSSA-based replication inhibitors, we examined conformational restrictions imposed by the [7,5]-azabicyclic lactam in the HCV NSSA inhibitor series and unexpectedly found bicyclic 5 to be nearly equipotent against HCV gt1b and only moderately less potent (~6×) against gt1a versus daclatasvir (1).<sup>13f</sup> Detailed molecular modeling of NSSA gt1a-docked 5 allowed us to postulate the binding mode for 5, in which the N-terminal substituent in 5 is reoriented toward a new site located between gt1a NSSA P97 and Y93 that is hard for 1 to access. Furthermore, aromatic amides were modeled to develop strong interactions with P97–Y93, suggesting facile ways to potentially improve the inhibitory potency against HCV by these analogues. Bicyclic rings of various sizes and substitutions in conjunction with the postulated amides create a substantial new chemistry space for further systematic explorations. It is tempting to examine whether molecules in this space can

bridge the unmet medical needs of patients that are not well served with current NSSA-based therapies, such as resistant or hard-to-treat HCV infections.<sup>9</sup> The results of our explorations in this space will be communicated in due time.

## ■ ASSOCIATED CONTENT

## SI Supporting Information

The Supporting Information is available free of charge at <https://pubs.acs.org/doi/10.1021/acsmmedchemlett.1c00391>.

Synthesis methods and experimental data for compounds, protocol for testing and data analysis of compounds in the HCV replicon assay, modeling methods, Supplemental Figure 1, and Supplemental Table 1 (PDF)

## ■ AUTHOR INFORMATION

## Corresponding Author

Wieslaw M. Kazmierski – GlaxoSmithKline, Research Triangle Park, North Carolina 27709-3398, United States; Present Address: Biohaven Pharmaceuticals, Inc., 215 Church Street, New Haven, CT 06510, United States; [orcid.org/0000-0002-5677-406X](https://orcid.org/0000-0002-5677-406X); Email: [wmk35860@gmail.com](mailto:wmk35860@gmail.com)

## Authors

**Nagaraju Miriyala** – GlaxoSmithKline, Research Triangle Park, North Carolina 27709-3398, United States; Present Address: UofL Health - Brown Cancer Center, University of Louisville, Louisville, KY 40202, United States; [orcid.org/0000-0002-1265-738X](https://orcid.org/0000-0002-1265-738X)

**David K. Johnson** – Computational Chemical Biology Core and Molecular Graphics and Modeling Laboratory, University of Kansas, Lawrence, Kansas 66047, United States; [orcid.org/0000-0003-4262-8173](https://orcid.org/0000-0003-4262-8173)

**Sam Baskaran** – GlaxoSmithKline, Research Triangle Park, North Carolina 27709-3398, United States; Present Address: Cellarity Inc., 100 Technology Square, Cambridge, MA 02139, United States; [orcid.org/0000-0002-2922-1670](https://orcid.org/0000-0002-2922-1670)

Complete contact information is available at:  
<https://pubs.acs.org/10.1021/acsmmedchemlett.1c00391>

## Author Contributions

#W.M.K. and N.M. contributed equally.

## Notes

The authors declare no competing financial interest.

## Biography

**Wieslaw “Wes” Kazmierski** received his Ph.D. in Organic Chemistry from the University of Arizona under the supervision of Professor Victor Hruby for his work on peptide mimetics. He was the founding scientist of the Selectide Corporation, where he codeveloped the One-Bead-One-Peptide concept. He codiscovered multiple clinical HIV and HCV small molecule inhibitors and modulators, including the drug Lexiva during his work at GlaxoSmithKline/ViiV Healthcare, where he was Scientific Leader and GSK Fellow. He is interested in new drug modalities, protein degradation, peptide therapies, antibody–drug conjugates, immunology, cancer research, and anti-infectives. He is currently Vice President of Chemistry at Biohaven Pharmaceuticals.

## ACKNOWLEDGMENTS

We thank our GSK colleagues for their expert contributions, data, and manuscript review. We also acknowledge support for the Computational Chemical Biology Core from the Chemical Biology of Infectious Disease Center of Biomedical Research Excellence (COBRE) through NIH Grant P20GM113117.

## REFERENCES

- (1) *Global Hepatitis Report, 2017*. World Health Organization, April 19, 2017. <https://www.who.int/publications/i/item/global-hepatitis-report-2017> (accessed 2020-04-30).
- (2) Macdonald, A.; Harris, M. Hepatitis C virus NSSA: tales of a promiscuous protein. *J. Gen. Virol.* **2004**, *85*, 2485–2502.
- (3) Moradpour, D.; Penin, F.; Rice, C. Replication of hepatitis C virus. *Nat. Rev. Microbiol.* **2007**, *5*, 453–463.
- (4) (a) Fukuma, T.; Enomoto, N.; Marumo, F.; Sato, C. Mutations in the interferon-sensitivity determining region of hepatitis C virus and transcriptional activity of the nonstructural region 5A protein. *Hepatology* **1998**, *28*, 1147–1153. (b) Fridell, R. A.; Qiu, D.; Valera, L.; Wang, C.; Rose, R. E.; Gao, M. Distinct functions of NSSA in hepatitis C virus RNA replication uncovered by studies with the NSSA inhibitor BMS-790052. *J. Virol.* **2011**, *85*, 7312–7320.
- (5) (a) Falade-Nwulia, O.; Suarez-Cuervo, C.; Nelson, D. R.; Fried, M. W.; Segal, J. B.; Sulkowski, M. S. Oral direct-acting agent therapy for hepatitis C virus infection. *Ann. Intern. Med.* **2017**, *166*, 637–648. (b) Spengler, U. Direct antiviral agents (DAAs) - a new age in the treatment of hepatitis C virus infection. *Pharmacol. Ther.* **2018**, *183*,

118–126. (c) Al-Salama, Z. T.; Deeks, E. D. Elbasvir/grazoprevir: a review in chronic HCV genotypes 1 and 4. *Drugs* **2017**, *77*, 911–921. (d) Lee, R.; Kottlil, S.; Wilson, E. Sofosbuvir/velpatasvir: a pangenotypic drug to simplify HCV therapy. *Hepatology International* **2017**, *11*, 161–170. (e) Lamb, Y. N. Glecaprevir/pibrentasvir: first global approval. *Drugs* **2017**, *77*, 1797–1804. (f) Struble, K.; Chan-Tack, K.; Qi, K.; Naeger, L. K.; Birnkrant, D. Benefit-risk assessment for sofosbuvir/velpatasvir/voxilaprevir based on patient population and hepatitis C virus genotype: U.S. food and drug administration's evaluation. *Hepatology (Hoboken, NJ, U. S.)* **2018**, *67*, 482–491. (g) Cheng, G.; Tian, Y.; Doehle, B.; Peng, B.; Corsa, A.; Lee, Y. J.; Gong, R.; Yu, M.; Han, B.; Xu, S.; Dvory-Sobol, H.; Perron, M.; Xu, Y.; Mo, H.; Pagratis, N.; Link, J. O.; Delaney, W. In vitro antiviral activity and resistance profile characterization of the hepatitis C virus NSSA inhibitor ledipasvir. *Antimicrob. Agents Chemother.* **2016**, *60*, 1847–1853.

(6) Pawlotsky, J. M. NSSA inhibitors in the treatment of hepatitis C. *J. Hepatol.* **2013**, *59*, 375–382.

(7) Sulkowski, M. S.; Vargas, H. E.; Di Bisceglie, A. M.; Kuo, A.; Reddy, K. R.; Lim, J. K.; Morelli, G.; Darling, J. M.; Feld, J. J.; Brown, R. S.; et al. Effectiveness of simeprevir plus sofosbuvir, with or without ribavirin, in real world patients with HCV genotype 1 infection. *Gastroenterology* **2016**, *150*, 419–429.

(8) Terrault, Z. S.; Zeuzem, S.; Di Bisceglie, A. M.; Lim, J. K.; Pockros, P. J.; Frazier, L. M. HCV-TARGET Study Group. Treatment outcomes with 8, 12 and 24-week regimens of ledipasvir/sofosbuvir for the treatment of hepatitis C infection: analysis of a multicenter prospective, observational study. Presented at the 66th Annual Meeting of the American Association for the Study of Liver Diseases, Boston, MA, November 13–17, 2015; Abstract 94.

(9) (a) Feld, J. J.; Foster, G. R. Second generation direct-acting antivirals – Do we expect major improvements? *J. Hepatol.* **2016**, *65*, S130–S142. (b) Bartenschlager, R.; Baumert, T. F.; Bukh, J.; Houghton, M.; Lemon, S. M.; Lindenbach, B. D.; Lohmann, V.; Moradpour, D.; Pietschmann, T.; Rice, C. M.; Thimme, R.; Wakita, T. *Virus Res.* **2018**, *248*, 53–62.

(10) (a) Kazmierski, W. M.; Maynard, A.; Duan, M.; Baskaran, S.; Botyanszki, J.; Crosby, R.; Dickerson, S.; Tallant, M.; Grimes, R.; Hamatake, R.; Leivers, M.; Roberts, C. D.; Walker, J. Novel spiroketal pyrrolidine GSK2336805 potently inhibits key hepatitis C virus genotype 1b mutants: from lead to clinical compound. *J. Med. Chem.* **2014**, *57*, 2058–2073. (b) Walker, J.; Crosby, R.; Wang, A.; Woldu, E.; Vamathevan, J.; Voitenleitner, C.; You, S.; Remlinger, K.; Duan, M.; Kazmierski, W.; Hamatake, R. Preclinical characterization of GSK2336805, a novel inhibitor of hepatitis C virus replication that selects for resistance in NSSA. *Antimicrob. Agents Chemother.* **2014**, *58*, 38–47.

(11) (a) Baskaran, S.; Kazmierski, W.; Duan, M.; Dickerson, S.; Cooper, J.; Grimes, R.; Walker, J. Novel naphthalene derivatives as potent HCV NSSA inhibitors for patients with chronic HCV infection: design, synthesis, SAR and optimization studies. Presented at the 248th ACS National Meeting & Exposition, San Francisco, CA, August 10–14, 2014; MEDI-407. (b) Kazmierski, W. M.; Adjabeng, G. M.; Baskaran, S.; Cooper, J.; Grimes, R.; Hamatake, R.; Leivers, M. R.; Meesala, R.; Nagaraju, M.; Walker, J. T. Discovery of GSK2818713, a novel second generation HCV NSSA replication complex inhibitor. Presented at the 251st ACS National Meeting & Exposition, San Diego, CA, March 13–17, 2016; MEDI-142. (c) Baskaran, S.; Grimes, R.; Kazmierski, W. M.; Leivers, M. R. Chemical compounds. US 8889726 B2, 2014. (d) Baskaran, S.; Grimes, R.; Kazmierski, W. M.; Leivers, M. R. Chemical Compounds. WO 2013022810, 2013. (e) Chen, P.; Couch, R.; Duan, M.; Grimes, R.; Kazmierski, W. M.; Norton, B. A.; Tallant, M. WO 2011028596 A1, 2011. (f) Kazmierski, W. M.; Baskaran, S.; Walker, J. T.; Miriyala, N.; Meesala, R.; Beesu, M.; Adjabeng, G.; Grimes, R. M.; Hamatake, R.; Leivers, M. R.; Crosby, R.; Xia, B.; Remlinger, K. *J. Med. Chem.* **2020**, *63*, 4155–4170.

(12) (a) Valle, G.; Kazmierski, W. M.; Crisma, M.; Bonora, G. M.; Toniolo, C.; Hruby, V. J. Constrained phenylalanine analogs.

Preferred conformation of the 1,2,3,4-tetrahydroisoquinoline-3-carboxylic acid (Tic) residue. *Int. J. Pept. Protein Res.* **1992**, *40*, 222–232. (b) Kummerle, A. E.; Vieira, M. M.; Schmitt, M.; Miranda, A. L. P.; Fraga, C. A. M.; Bourguignon, J.-J.; Barreiro, E. J. Design, synthesis and analgesic properties of novel conformationally-restricted *N*-acylhydrazones (NAH). *Bioorg. Med. Chem. Lett.* **2009**, *19*, 4963–4966. (c) Hanessian, S.; Auzzas, L. The practice of ring constraint in peptidomimetics using bicyclic and polycyclic amino acids. *Acc. Chem. Res.* **2008**, *41*, 1241–1251. (d) Fang, Z.; Song, Y.; Zhan, P.; Zhang, Q.; Liu, X. Conformational restriction: an effective tactic in “follow-on”-based drug discovery. *Future Med. Chem.* **2014**, *6*, 885–901. (e) Ikegashira, K.; Oka, T.; Hirashima, S.; Noji, S.; Yamanaka, H.; Hara, Y.; Adachi, T.; Tsuruha, J.; Doi, S.; Hase, Y.; Noguchi, T.; Ando, I.; Ogura, N.; Ikeda, S.; Hashimoto, H. Discovery of conformationally constrained tetracyclic compounds as potent hepatitis C virus NS5B RNA polymerase inhibitors. *J. Med. Chem.* **2006**, *49*, 6950–6953. (f) Stansfield, I.; Ercolani, C.; Mackay, A.; Conte, I.; Pompei, M.; Koch, U.; Gennari, N.; Giuliano, C.; Rowley, M.; Narjes, F. Tetracyclic indole inhibitors of hepatitis C virus NS5B-polymerase. *Bioorg. Med. Chem. Lett.* **2009**, *19*, 627–632. (g) Coburn, C. A.; Meinke, P. T.; Chang, W.; Fandozzi, C. M.; Graham, D. J.; Hu, B.; Huang, Q.; Kargman, S.; Kozlowski, J.; Liu, R.; McCauley, J. A.; Nomeir, A. A.; Soll, R. M.; Vacca, J. P.; Wang, D.; Wu, H.; Zhong, B.; Olsen, D. B.; Ludmerer, S. W. Discovery of MK-8742: an HCV NS5A inhibitor with broad genotype activity. *ChemMedChem* **2013**, *8*, 1930–1940. (h) Zheng, Y.; Tice, C. M.; Singh, S. B. The use of spirocyclic scaffolds in drug discovery. *Bioorg. Med. Chem. Lett.* **2014**, *24*, 3673–3682.

(13) (a) Tsantrizos, Y. Peptidomimetic therapeutic agents targeting the protease enzyme of the human immunodeficiency virus and hepatitis C virus. *Acc. Chem. Res.* **2008**, *41*, 1252–1263. (b) Ramsis, T. M.; Abdel Karim, S. E.; Vassilaki, N.; Frakolaki, E.; Kamal, A. A. M.; Zoidis, G.; Ahmed, N. S.; Abadi, A. H. Expanding the chemical space of anti-HCV NS5A inhibitors by stereochemical exchange and peptidomimetic approaches. *Arch. Pharm.* **2018**, *351*, No. 1800017. (c) Leila, A. R. S.; Mousa, M. H. A.; Frakolaki, E.; Vassilaki, N.; Bartenschlager, R.; Zoidis, G.; Abdel-Halim, M.; Abadi, A. H. Symmetric anti-HCV agents: synthesis, antiviral properties, and conformational aspects of core scaffolds. *ACS Omega* **2019**, *4*, 11440–11454. (d) Sun, H.; Nikolovska-Coleska, Z.; Yang, C. Y.; Xu, L.; Liu, M.; Tomita, Y.; Pan, H.; Yoshioka, Y.; Krajewski, K.; Roller, P. P.; Wang, S. Symmetric anti-HCV agents: synthesis, antiviral properties, and conformational aspects of core scaffolds. *J. Am. Chem. Soc.* **2004**, *126*, 16686–16687. (e) Chang, W.; Mosley, R. T.; Bansal, S.; Keilman, M.; Lam, A. M.; Furman, P. A.; Otto, M. J.; Sofia, M. J. Inhibition of hepatitis C virus NS5A by fluoro-olefin based  $\gamma$ -turn mimetics. *Bioorg. Med. Chem. Lett.* **2012**, *22*, 2938–2942. (f) Wakenhut, F.; Tran, T. D.; Pickford, C.; Shaw, S.; Westby, M.; Smith-Burchnell, C.; Watson, L.; Paradowski, M.; Milbank, J.; Stonehouse, D.; Cheung, K.; Wybrow, R.; Daverio, F.; Crook, S.; Statham, K.; Leese, D.; Stead, D.; Adam, F.; Hay, D.; Roberts, L. R.; Chiva, J.-Y.; Nichols, C.; Blakemore, D. C.; Goetz, G. H.; Che, Y.; Gardner, I.; Dayal, S.; Pike, A.; Webster, R.; Pryde, D. C. The discovery of potent NS5A inhibitors with a unique resistance profile part 2. *ChemMedChem* **2014**, *9*, 1387–1396.

(14) (a) Gosselin, F.; Lubell, W. D. Rigid dipeptide surrogates: syntheses of enantiopure quinolizidinone and pyrroloazepinone amino acids from a common diaminodicarboxylate precursor. *J. Org. Chem.* **2000**, *65*, 2163–2171. (b) Buckman, B.; Nicholas, J. B.; Serebryany, V.; Seiwert, S. D. WO 2011/146401 A1, 2011.

(15) Belema, M.; Nguyen, V. N.; Bachand, C.; Deon, D. H.; Goodrich, J. T.; Lavoie, R.; James, C. A.; Lopez, O. D.; Martel, A.; Romine, J. L.; et al. Hepatitis C virus NS5A replication complex inhibitors: the discovery of daclatasvir. *J. Med. Chem.* **2014**, *57*, 2013–2032.

(16) Belema, M.; Nguyen, V. N.; Romine, J. L.; St. Laurent, D. R.; Lopez, O. D.; Goodrich, J.; Nower, P. T.; O’Boyle, D. R., II; Lemm, J. A.; Fridell, R. A.; Gao, M.; Fang, H.; Krause, R. G.; Wang, Y.-K.; Oliver, A. J.; Good, A. C.; Knipe, J. O.; Meanwell, N. A.; Snyder, L. B.

Hepatitis C virus NS5A replication complex inhibitors. Part 6: the discovery of a novel and highly potent biarylimidazole chemotype with inhibitory activity toward genotype 1a and 1b replicons. *J. Med. Chem.* **2014**, *57*, 1995–2012. For compound **50c**, the gt1a and gt1b IC<sub>50</sub> values were 0.037 and 0.042 nM, respectively.

(17) Lambert, S. M.; Langley, D. R.; Garnett, J. A.; Angell, R.; Hedgethorne, K.; Meanwell, N. A.; Matthews, S. J. The crystal structure of NS5A domain 1 from genotype 1a reveals new clues to the mechanism of action for dimeric HCV inhibitors. *Protein Sci.* **2014**, *23*, 723–734.

(18) Love, R. A.; Brodsky, O.; Hickey, M. J.; Wells, P. A.; Cronin, C. N. Crystal structure of a novel dimeric form of NS5A domain I protein from hepatitis C virus. *J. Virol.* **2009**, *83*, 4395–4403.

(19) Gao, M.; Nettles, R. E.; Belema, M.; Snyder, L. B.; Nguyen, V. N.; Fridell, R. A.; Serrano-Wu, M. H.; Langley, D. R.; Sun, J.-H.; O’Boyle, D. R., II; Lemm, J. A.; Wang, C.; Knipe, J. O.; Chien, C.; Colonno, R. J.; Grasela, D. M.; Meanwell, N. A.; Hamann, L. G. Chemical genetics strategy identifies an HCV NS5A inhibitor with a potent clinical effect. *Nature* **2010**, *465*, 96–100.

(20) Friesner, R. A.; Banks, J. L.; Murphy, R. B.; Halgren, T. A.; Klicic, J. J.; Mainz, D. T.; Repasky, M. P.; Knoll, E. H.; Shelley, M.; Perry, J. K.; Shaw, D. E.; Francis, P.; Shenkin, P. S. Glide: a new approach for rapid, accurate docking and scoring. 1. Method and assessment of docking accuracy. *J. Med. Chem.* **2004**, *47*, 1739–1749.

(21) Friesner, R. A.; Murphy, R. B.; Repasky, M. P.; Frye, L. L.; Greenwood, J. R.; Halgren, T. A.; Sanschagrin, P. C.; Mainz, D. T. Extra precision glide: docking and scoring incorporating a model of hydrophobic enclosure for protein-ligand complexes. *J. Med. Chem.* **2006**, *49*, 6177–6196.

(22) Halgren, T. A.; Murphy, R. B.; Friesner, R. A.; Beard, H. S.; Frye, L. L.; Pollard, W. T.; Banks, J. L. Glide: a new approach for rapid, accurate docking and scoring. 2. Enrichment factors in database screening. *J. Med. Chem.* **2004**, *47*, 1750–1759.

(23) Manzoni, L.; Colombo, M.; May, E.; Scolastico, C. Synthesis of spiroazabicycloalkane amino acid scaffolds as reverse-turn inducer dipeptide mimics. *Tetrahedron* **2001**, *57*, 249–255.

(24) Angiolini, M.; Araneo, S.; Belvisi, L.; Cesarotti, E.; Checchia, A.; Crippa, L.; Manzoni, L.; Scolastico, C. Synthesis of azabicycloalkane amino acid scaffolds as reverse-turn inducer dipeptide mimics. *Eur. J. Org. Chem.* **2000**, *2000*, 2571–2581.